Cell Detection and Segmentation in Microscopy Images with Improved Mask R-CNN

Seiya Fujita[1] and Xian-Hua Han[1][0000−0002−5003−3180]

Graduate School of Science and Technology for Innovation, Yamaguchi University, 1677-1 Yoshida, Yamaguchi City, Yamaguchi, 753-8511, Japan.
b026vb@yamaguchi-u.ac.jp
hanxhua@yamaguchi-u.ac.jp

Abstract. Analyzing and elucidating the attributes of cells and tissues with an observed microscopy image is a fundamental task in both biological research and clinical practice, and automation of this task to develop computer aided system based on image processing and machine learning technique has been rapidly evolved for providing quantitative evaluation and mitigating burden and time of the biological experts. Automated cell/nuclei detection and segmentation is in general a critical step in automatic system, and is quite challenging due to the existed heterogeneous characteristics of cancer cell such as large variability in size, shape, appearance, and texture of the different cells. This study proposes a novel method for simultaneous detection and segmentation of cells based on the Mask R-CNN, which conducts multiple end-to-end learning tasks by minimizing multi task losses for generic object detection and segmentation. The conventional Mask R-CNN employs cross entropy loss for evaluating the object detection fidelity, and equally treats all training samples in learning procedure regardless to the properties of the objects such as easily or hard degree for detection, which may lead to miss-detection of hard samples. To boost the detection performance of hard samples, this work integrates the focal loss for formulating detection criteria into Mask R-CNN, and investigate a feasible method for balancing the contribution of multiple task losses in network training procedure. Experiments on the benchmark dataset: DSB2018 manifest that our proposed method achieves the promising performance on both cell detection and segmentation.

1 Introduction

With the development of whole slide digital scanning technology, it is now possible to digitize and store tissue slides in digital image format. Manual analysis of these microscopy images can be very burdensome and time-consuming for professionals. Automated analysis of these types of images to provide quantitative measurements has received a lot of attention and has contributed significantly to the advancement of computer-assisted diagnostic systems. One of the key tasks in cellular image analysis is to identify certain grades (e.g., cancer) or different types of tumors related to the degree of cellular heterogeneity involved in tumor

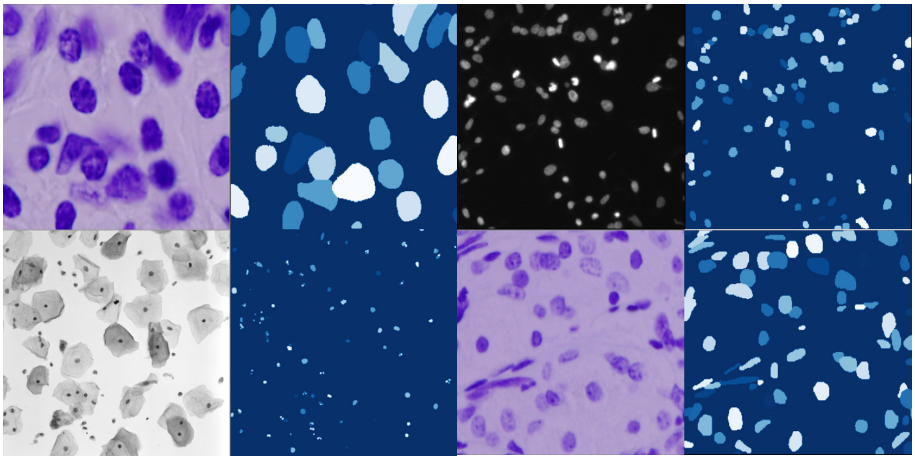

Fig. 1. Some examples of the microscopy images and their corresponding masks in DSB2018 dataset. It is obvious that the variety of the microscopy image is substantial large and would be a very challenge task for cell detection and segmentation.

development. In this context, the recognition and detection of cell nuclei is an important step for detailed cellular analysis in computer-assisted diagnostic systems. In addition, shape recognition of cell nuclei is an important task in grade discrimination of the species or identifying whether the tumor is of a different type.

Therefore, localization of different cells and pixel-wise recognition to obtain the precise shape of cell nuclear is a crucial step for most downstream tasks, and meanwhile is very difficult due to the existing heterogeneous characteristics of cancer cells, such as large variations in size, shape, appearance, color of stain, and texture of various cells. Figure 1 manifests some examples of the microscopy images and the annotated masks in DSB2018 dataset. This simultaneous detection/localization and segmentation of an object in computer vision field are well known as instance segmentation involving the assignment of instance identity to every pixel in the image. This study aims at instance segmentation of cell nuclei.

Most instance segmentation approaches follow separate detection and segmentation paradigm, which firstly employs state-of-the art object detection methods to extract the bounding box of each object and then conducts segmentation on each bounding box. For object detection, there are mainly two types of deep learning based methods: single stage detection frameworks such as SSD [8] and YOLO [9], and two stage detection frameworks [4] such as Faster R-CNN [5]. Single stage method treats object detection as a simple regression problem via simultaneously learning the class probabilities and bounding box coordinates from an input image in a single step while two stage detector firstly estimates candidate regions using a region proposal network and then performs object classification and bounding-box regression for the region proposals. Such models generally achieve higher accuracy rates, but are typically slower than single

stage detector. Segmentation is implemented on the detected objects for providing the final instance segmentation results. However, such pipeline conducts object detection and the downstream segmentation independently, and may lead to sub-optimal results. He et al. [6] proposed a simple, flexible and general end-to-end learning network for instance segmentation, called as Mask R-CNN. Mask R-CNN extends Faster R-CNN by adding a prediction branch of an object mask in parallel with the bounding box regression branch in the raw faster R-CNN, and has been proven the applicability for different detection/localization and segmentation tasks. [1–3]

This study adopts Mask R-CNN for simultaneously cell detection and segmentation. It is well known that the model training of Mask R-CNN involves minimization of several loss functions for the multiple task learning tasks. However, how different losses contribute to the final detection and segmentation results remains un-exploration. This work investigates the impact of different losses used in Mask R-CNN via adjusting the weights of different losses. In addition, conventional Mask R-CNN employs cross entropy loss for evaluating the object detection fidelity, and equally treats all training samples in learning procedure regardless to the properties of the objects such as easy or hard degree for detection, which may lead to miss-detection of hard samples. To boost the detection performance of hard samples, we integrate the focal loss [7] for formulating detection criteria into Mask R-CNN, and investigate a feasible method for balancing the contribution of multiple task losses in network training procedure. Experiments on the benchmark dataset: DSB2018 manifests that our proposed method achieves the promising performance on both cell detection and segmentation.

The rest of this paper is organized as follows. Section 2 surveys the related work including cell detection method and segmentation approach. Section 3 presents the strategy for exploring the effect of different losses to the detection and segmentation results and the integration of the focal loss into Mask R-CNN. Extensive experiments are conducted in Sec. 4 to compare the proposed method with the baseline Mask R-CNN on DSB2018 datasets. Conclusion is given in Sec. 5.

2 Related work

In the past few years, cell detection and segmentation has been actively research in computer vision and medical image processing community, and substantial improvement have been witnessed. This work concentrates on simultaneously detection and segmentation of cells in microscopy images. Here, we briefly survey the related work about cell detection and segmentation, respectively.

2.1 Cell detection approaches

Different cell recognition and detection methods for computer-aided diagnosis systems have been explored, and many methods mainly employ traditional

paradigm via extracting hand-crafted feature representation and conducting classification independently. For example, Humayun et al. [10] proposed to using morphological and multi-channel statistics features for mitosis detection. Al-kofahi et al. [11] explored multiscale Laplacian-of-Gaussian filtering for nuclear seed point detect. Meanwhile Gabor filter or LBP feature [12] provides a lot of interesting texture properties and had been popularly applied for a cell detection task. Although the traditional cell detection paradigm has been widely researched, the independent procedure for hand-crafted feature extraction and classification suffer from several limitations; 1) it is difficult to select proper features for different tasks; 2) different features are needed to be designed for representing various aspects of the input; 3) the separation using of feature extraction and classification generally leads to sub-optimal results for the under-studying tasks.

Recently, motivated by the successes of the deep learning on computer vision community, deep convolutional neural network has popularly been used for cell detection and localization. [13] initially applied a fully convolutional network for cell counting via predicting a spatial density map of target cell and then estimating the cell number with an integration over the learned density map. Later, Chen et al. [14] proposed a cascaded network for cell detection which firstly uses the FCN for candidate region selection and then adopts another CNN for classifying the candidate regions and background. Meanwhile [15] investigated a CNN-based prediction method following by ad-hoc post processing, which trains CNN model to classify each pixel represented with a patch centered on the pixel and then conducts post processing on the network output. Shadi et al. [16] employed expectation maximization with deep learning framework in an end-to-end manner for cell detection, which can handle the learning task from crowds via leveraging an additional crowd-sourcing layer on the CNN architecture. More recently, Xue et al. [17] combined deep CNN with compressed sensing for cell detection and Schmidt et al. [18] proposed to localize cell nuclei via star-convex polygons for better shape representation than the conventional bounding box. In spite of the promising performance, the cell detection method cannot provide detailed shape of the cell which may be necessary for the downstream tasks.

2.2 Cell segmentation

To analyze the characteristics of each individual cell, cell segmentation is an essential step in different microscopy image analysis systems, and many methods have been proposed. One of the most common methods for this task is to simply use intensity thresholding, and usually suffers from intensity inhomogeneity. To separate touching and overlapping cell and nuclei, watershed-based [20, 21] and level-set methods [22, 23] have been applied for cell segmentation. Dorini et al. [24] proposed to employ morphological operators and scale-space analysis for white blood cell segmentation, which assumes a blob-like shape of the cell nucleus to conduct blob-based detection as the initialization of a graph-based method while Wang et al. explored snake algorithm for cell segmentation and tracking.

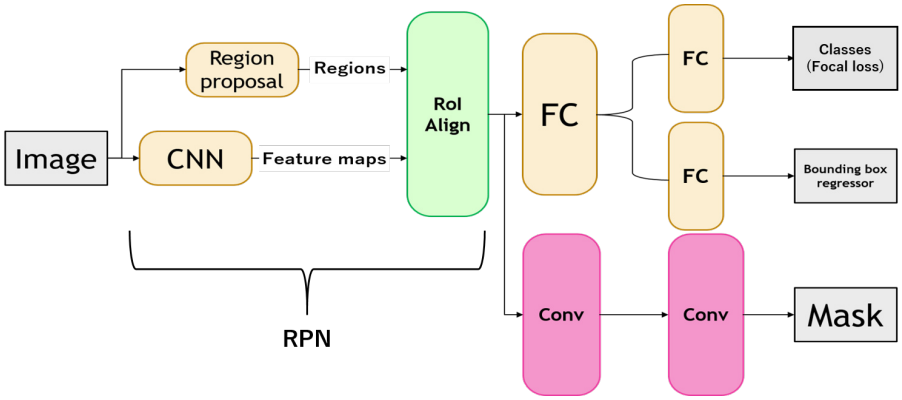

Fig. 2. The schematic concept of the Mask R-CNN for simultaneous object detection and segmentation via adding a branching subnet to Faster R-CNN to estimate the segmentation mask, which is itself a multitask learning framework with multiple loss functions.

Recently, deep convolutional network has been proven to be very effective for segmentation of different types of images, and has also been applied for the segmentation of cell nuclei [25–27]. In 2015, the encoder-decoder framework: U-Net architecture was developed specifically for the segmentation of medical images, and applied on the ISBI challenge for segmentation of neuronal structures in electron microscopy stacks to produce state-of-the-art results [28]. Since then, U-Net has been used for a wide range of tasks in medical image analysis including cell segmentation and tracking on time-lapse microscopy images [29]. More recently, Mask R-CNN [6] has been proposed to extend the Faster R-CNN [5] model for simultaneous object localization and instance segmentation of natural images, and has also been adapted for cell localization and single cell segmentation. Due to the property of multi-task learning in the Mask R-CNN, it entails the use of multi-task loss functions for training the end-to-end learning network. However, how different losses contribute to the final results remains un-exploration, and balance of the multi-task losses for various applications may be a non-trivial step. This study also follows the paradigm of Mask R-CNN for segmentation of individual cells. We extensively explore the effect of different losses on the final detection and segmentation results.

3 Method

Mask R-CNN enables instance segmentation by adding mask branches to the head of the Faster R-CNN network, which allows segmentation of each detected object. In this study, we adapt Mask R-CNN to simultaneously detect and segment cell nuclei in microscopy images. The schematic concept of the Mask R-CNN is show in Fig. 2. To conduct simultaneous object detection and segmentation, Mask R-CNN is itself a multi-task learning framework, and consists of

multiple losses for training the end-to-end network. However, contributions of different losses to the final results remains un-exploration, and it is still unclear how to select the proper weights (hyper-parameters) of the used multiple losses for boosting the performance of the under-studying target. This study proposes a weight-selection strategy for exploring the effect of different losses to the final prediction. In addition, conventional Mask R-CNN uses cross entropy loss to assess the fidelity of object detection and treats all training samples in the training procedure equally, regardless of object properties such as the degree of ease or difficulty of detection, and has shown high accuracy results in general object detection. However, cell nucleus detection is very difficult due to the heterogeneous properties of various images, including large variations in size, shape, appearance, staining and texture. Therefore, we propose to improve the accuracy by using focal loss instead of cross entropy loss. Next, we present the detail description of the adaptive weight-selection strategy and the focal-loss based Mask R-CNN.

3.1 Weight-selection strategy

To implement multiple tasks, Mask R-CNN employs multiple losses, which consisting of the losses: ($L_{Class_{RPN}}$ and $L_{Bbox_{RPN}}$) in the RPN subnet for extracting objectness regions and the final class prediction losses: class loss (L_{Class}) for classifying objectness regions into different classes, Bbox loss (L_{Bbox}) for estimating the bounding box of objects and mask loss (L_{Mask}) for segmenting individual object, to learn the shared network parameters. The loss functions of Mask R-CNN can be expressed as:

$$Loss_{total} = L_{Class_{RPN}} + L_{Bbox_{RPN}} + \alpha L_{Class} + \beta L_{Bbox} + L_{Mask} \qquad (1)$$

Mask R-CNN empirically set the hyper-parameters α and β as 1, and concurrently minimize all losses for implementing the multitask learning, where different losses may lead to different degrees of learning. For instance, the loss function with smaller value may serve little to network learning while loss with large value would give great effect to the network parameter updating. From Eq. (1), it can be seen that Mask R-CNN losses can be divided into RPN losses and prediction losses for final results. Since the RPN losses mainly aid to obtain the initial object candidates for being forwarded to the subsequent prediction procedure, it is usually considered to have no great effect on the final prediction results according to our experience and observation. This work concentrates on exploring the weight-selection strategy for the hyper-parameters α and β in Eq. (1) for adaptively selecting the weight of the prediction losses: L_{Class}, L_{Bbox} and L_{Mask}. Figure 3. (a) plots the values of different prediction losses with different epoch numbers in training procedure, which manifests the different values among the three prediction losses. Since the three losses contribute to various tasks: classification, segmentation and bounding box regression, respectively, smaller value of one loss may lead to not-enough learning for the corresponding task and then possibly results in adverse effect on other tasks. Thus we propose a weight-selection strategy to adaptively adjust the weights: α and β in network training

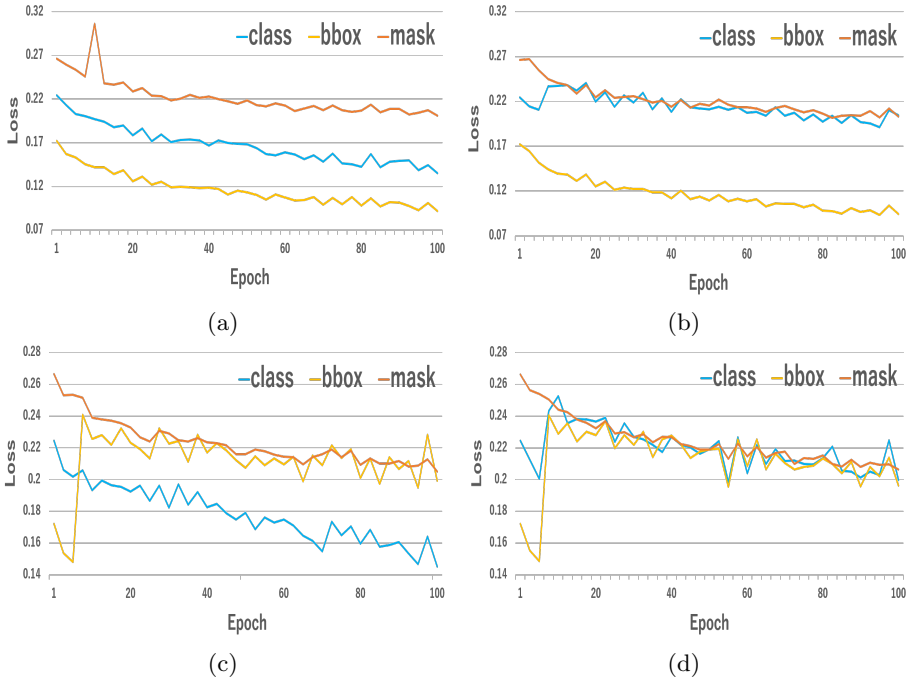

Fig. 3. The values of different predicted Losses in conventional Mask R-CNN, and the proposed models with the weight-selection strategy for updating α or β or both weights. a) Mask R-CNN; b) Weight updating for α; c) Weight updating for β; d) Weight updating for both α and β.

procedure, and update these weights at each epoch according to the loss values of the previous epoch. The updating of the weights: α and β is formulated as the following:

$$\alpha_{t+1} = \frac{\max(L_{Class}, L_{Bbox}, L_{Mask})}{L_{Class}}\alpha_t \tag{2}$$

$$\beta_{t+1} = \frac{\max(L_{Class}, L_{Bbox}, L_{Mask})}{L_{Bbox}}\beta_t \tag{3}$$

$$Loss_{total_{t+1}} = L_{Class_{RPN}} + L_{Bbox_{RPN}} + \alpha_{t+1}L_{Class} + \beta_{t+1}L_{Bbox} + L_{Mask} \tag{4}$$

Where α_t and β_t are the weights at the t-th epoch while α_{t+1} and β_{t+1} are the updated weights at the $(t+1)$-th epoch. We firstly set the initial weights at the first epoch as $\alpha_1 = 1$, $\beta_1 = 1$, and update them at each epoch in network training procedure.

3.2 Focal-loss based Mask R-CNN

Due to the heterogeneous properties of microscopy images such as large variations in size, shape, appearance, staining and texture, there exist some difficult

cell instances to be detected and recognized. We integrate focal loss for object classification instead of cross entropy loss into Mask R-CNN. Focal loss attenuates the effect of the losses obtained from large amount of easy samples while emphasizes the contribution of losses obtained from small proportion of hard samples that are difficult to be recognized. Thus This makes it possible to increase the loss for cell nuclei that are difficult to be distinguished in the microscopy images and decrease the loss for cell nuclei that are easy to be distinguished. Let denotes the predicted probability of a training sample as P_T on the ground truth class T, the focal loss calculated from this sample can be formulated as:

$$L_{FocalLoss} = -\delta(1 - P_T)^{\gamma} \log P_T \tag{5}$$

where δ, γ are hyper-parameters with δ controlling the contribution of the whole focal loss to the total loss while γ adjusting the contribution of each individual cell according to the classification difficulty. In this study, we set $\gamma = 1$. From Eq. (5), it can be seen that the value of the focal loss without considering the effect of the controlling hyper-parameter δ, would become smaller than the value of the cross-entropy loss: $-P_T log P_T$ for most samples, which would weaken the learning degree of the object classification task compared to other tasks. Thus we propose an automatic regulating method for designing the hyper-parameter δ to balance the focal loss with other losses. The automatic regulating method for updating δ at each epoch in network training procedure is formulated as:

$$\delta_{t+1} = \frac{\max(L_{FocalLoss}, L_{Bbox}, L_{Mask})}{L_{FocalLoss}} \delta_t \tag{6}$$

where δ_t and δ_{t+1} denote the weights in the t-th and $(t+1)$-th epochs, respectively.

4 Experiments results

4.1 Dataset

To evaluate the effectiveness of our proposed method, we conducted experiments on the 2018 Data Science Bowl dataset (DSB2018). DSB2018 dataset has in total 670 microscopy images captured in various modalities, and therein 645 images were used for training and 25 were used for testing. We also conducted data augmentation via left/right flipping, up/down flipping, rotation, Gaussian blurring and darkening operations on the raw images in training procedure.

4.2 Evaluation Metric

We adopt $F1$ *measure* to evaluating the performance of object detection. A detected object I_{pred} is considered as a proper match (*true positive* TP_τ) if a ground truth object I_{gt} exists whose *intersection over union* : $IoU = \frac{I_{pred} \cap I_{gt}}{I_{pred} \cup I_{gt}}$

with the prediction is greater than a given threshold $\tau \in [0, 1]$. Unmatched predicted objects are counted as $false\ positives$ (FP_τ) while unmatched ground truth objects are as $false\ negatives$ (FN_τ). Given the matching evaluations: TP_τ, FP_τ and FN_τ, the evaluation metrics: $Precision$ for measuring prediction accuracy and $Recall$ for measuring the reproducibility of forecasts are formulated as:

$$Precision = \frac{TP_\tau}{TP_\tau + FP_\tau}, Recall = \frac{TP_\tau}{TP_\tau + FN_\tau} \tag{7}$$

Then the $F1\ measure$ is expressed by the following equation:

$$F1measure = 2\frac{Precision * Recall}{Precision + Recall} \tag{8}$$

For segmentation evaluation, we use $Dice$ metric. The segmented results are evaluated pixel by pixel to calculate TP, FP, and FN, and then $Precision_d$ and $Recall_d$ are computed based on Eq. (7). Finally the $Dice$ is calculated as:

$$Dice = 2\frac{Precision_d * Recall_d}{Precision_d + Recall_d}. \tag{9}$$

4.3 Performance comparison

We conducted experiments with different models for simultaneous cell detection and segmentation and provide the compared results.

Comparison of Mask R-CNN models w/o the weight-selection strategy: As described in Sec. 3, we explored a weight-selection strategy for adaptively adjusting the hyper-parameters of different prediction losses in Mask R-CNN. Initially, we set the hyper-parameters (weights) in Eq. (1) as $\alpha_1 = 1$, $\beta_1 = 1$, and then update the parameters according to Eq. (2) and (3). We implemented four models: Mask R-CNN without the weight-selection strategy, the other three models with the updating for only α or β or both. The values of different losses for the three improved models are shown in Fig. 3(b), (c) and (d). The compared results are given in Table 1, which manifests the updating of α for re-weighting the class loss achieves best performance. From the results in Table 1, it can be concluded that the class loss for classifying the cell candidate regions has more contribution to the final performance.

Comparison of the focal-loss based Mask R-CNN: We integrated the focal loss into Mask R-CNN for evaluating cell detection and segmentation performance. Compared with the cross-entropy loss, the value of the focal loss would become smaller, and thus we explore a method for automatically designing the contributed weight in Eq. (6). The compared results are provided with the following 4 models: 1) the conventional Mask R-CNN; 2) Mask R-CNN + FL ($\alpha = 1$) via integrating the focal loss with the weight $\alpha = 1$; 2) Mask R-CNN + FL ($\alpha = 5$) via integrating the focal loss with the weight $\alpha = 5$; 4) Mask R-CNN + FL (Balanced) via integrating the focal loss with automatically regulated weight. In all models, we set the NMS threshold as 0.3 for detecting cell candidates, and

Table 1. Compared cell detection and segmentation results w/o the weight-selection strategy.

	$Loss_{Class}$	$Loss_{Bbox}$	τ =0.50	0.55	0.60	0.65	0.70	0.75	0.80	0.85	0.90	*Dice*
MRCNN	-	-	0.77	0.75	0.72	0.68	0.63	0.56	0.45	0.28	0.09	0.877
Class	✓	-	0.79	0.77	0.75	0.71	0.65	0.59	0.45	0.27	0.07	0.880
Bbox	-	✓	0.77	0.75	0.74	0.70	0.65	0.57	0.46	0.26	0.08	0.878
Class_Bbox	✓	✓	0.74	0.73	0.70	0.67	0.61	0.53	0.43	0.26	0.07	0.878

Table 2. Nuclei detection results, showing $F1$ *measure* for several *intersection over union* (IoU) thresholds τ, and segmentation results *Dice*.

Threshold τ	0.50	0.55	0.60	0.65	0.70	0.75	0.80	0.85	0.90	Dice
Mask R-CNN	0.77	0.75	0.72	0.68	0.63	0.56	0.45	0.28	0.09	0.877
MRCNN + FL($\alpha = 1$)	**0.81**	**0.79**	**0.76**	**0.72**	**0.67**	**0.60**	**0.48**	**0.31**	**0.11**	**0.888**
MRCNN + FL($\alpha = 5$)	0.78	0.74	0.71	0.67	0.63	0.55	0.43	0.27	0.10	0.871
MRCNN + FL(*balanced*)	0.78	0.76	0.73	0.70	0.65	0.57	0.45	0.28	0.09	0.883

the score threshold as 0.5 for cell classification. We used the pre-trained ResNet with ImageNet dataset as the backbone network, and then perform the transfer training for cell detection and segmentation. The compared results with the four models are shown in Table 2. Table 2 manifests the model with the focal loss and the weight α =1 achieved best performance for both cell detection and segmentation. In our experiments, there are in total 1504 ground truth cells in the 25 test microscopy images, and the detected cell number with the threshold $\tau = 0.5$ by the four models: Mask R-CNN, Mask R-CNN + FL ($\alpha = 1$), Mask R-CNN + FL ($\alpha = 5$) and Mask R-CNN + FL (Balanced) are 1109, 1277, 1209 and 1128, respectively, which means that the integration of the focal loss can increase the number of detected cells. The Dice values in Table 2 are calculated for the detected cell nuclei. Finally, we give the visualization results of several microscopy images in Fig. 4, which also manifests some improvement with the integration of the focal loss in the Mask R-CNN.

5 Conclusion

In this study, we adopted Mask R-CNN to simultaneously detect and segment cell nuclei in a microscopy image, which is the most popular deep learning-based method for instance segmentation of natural images. Specifically, due to the multi-task learning property of the Mask R-CNN, we proposed a weight-selection strategy for adaptively adjusting the hyper-parameters of different prediction losses, and evaluated the effect of different losses to the final prediction for cell detection and segmentation. Further, we integrated the focal loss into Mask R-CNN for concentrating the hard samples to be recognized and meanwhile investigated an automatic regulating method for calculating the contributed weight of the focal loss. Experimental results on DSB2018 validated that our proposed

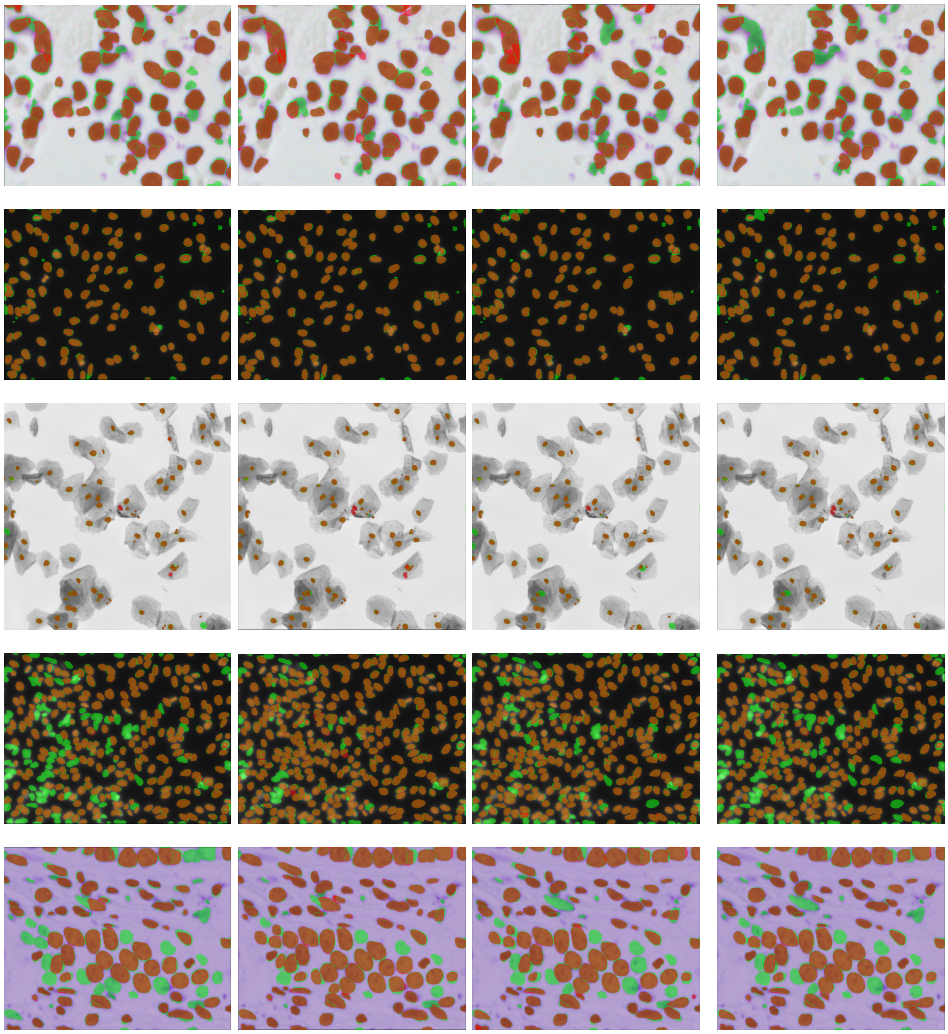

Mask R-CNN MRCNN+FL($\alpha = 1$) MRCNN+FL($\alpha = 5$) MRCNN+FL(Balance)

Fig. 4. Compared cell detection and segmentation results using the conventional Mask R-CNN and the focal-loss based Mask R-CNN. Green color represents GT pixels, Red color represents predicted cell pixels and Brown color denotes the overlapped regions of GT and prediction.

model can improve performance of both cell detection and segmentation compared with the baseline Mask R-CNN.

6 ACKNOWLEDGE

This research was supported in part by the Grant-in Aid for Scientific Research from the Japanese Ministry for Education, Science, Culture and Sports (MEXT) under the Grant No. 20K11867.

References

1. Rajaram Anantharaman, Matthew Velazquez, Yugyung Lee, "Utilizing Mask R-CNN for Detection and Segmentation of Oral Diseases", IEEE International Conference on Bioinformatics and Biomedicine, 2018
2. Jeremiah W. Johnson, "Automatic Nucleus Segmentation with Mask R-CNN" CVC 2019, Advances in Computer Vision pp 399-407
3. Chengjun Tan, Nasim Uddin, Yahya M. Mohammed, "Deep Learning-Based Crack Detection Using Mask R-CNN Technique" 9th International Conference on Structural Health Monitoring of Intelligent Infrastructure
4. R. Girshick, "Fast R-CNN," IEEE International Conference on Computer Vision (ICCV), 2015.
5. Shaoqing Ren, Kaiming He, Ross Girshick, and Jian Sun. "Faster R-CNN: Towards real-time object detection with region proposal networks", Advances in neural information processing systems, pp. 91–99, 2015.
6. Kaiming He, Georgia Gkioxari, Piotr Dollar, and Ross Girshick. "Mask R-CNN". In ICCV, 2017.
7. Tsung-Yi Lin, Priya Goyal, Ross Girshick, Kaiming He, and Piotr Dollar. "Focal loss for Dense Object Detection". In ICCV, 2017.
8. Wei Liu, Dragomir Anguelov, Dumitru Erhan, Christian Szegedy, Scott Reed,Cheng-Yang Fu, Alexander C. Berg, "SSD: Single Shot MultiBox Detector", Computer Vision - ECCV 2016 pp.21- 37, 2016.
9. J. Redmon, S. Divvala, R. Girshick, and A. Farhadi. "You only look once: Unified, real-time object detection." arXiv preprint arXiv:1506.02640, 2015.
10. Humayun Irshad "Automated mitosis detection in histopathology using morphological and multi-channel statistics features" Journal of Pathology Informatics ,2013
11. Yousef Al-Kofahi, Wiem Lassoued, William Lee, Badrinath Roysam, "Improved automatic detection and segmentation of cell nuclei in histopathology images" IEEE Transactions on Biomedical Engineering, 2009
12. Timo Ojala, Matti Pietikainen, David Harwood, "A comparative study of texture measures with classification based on feature distributions" Pattern Recognition, 29 (1996), pp. 51-59
13. Weidi Xie, J. Alison Noble, Andrew Zisserman "Microscopy Cell Counting with Fully Convolutional Regression Networks" Computer Methods in Biomechanics and Biomedical Engineering: Imaging & Visualization, 283-292, 2018
14. Hao Chen, Qi Dou, Xi Wang, Jing Qin, Pheng-Ann Heng, "Mitosis detection in breast cancer histology images via deep cascaded networks." AAAI'16: Proceedings of the Thirtieth AAAI Conference on Artificial Intelligence, 1160-1166, 2016

15. Dan C. Cireşan, Alessandro Giusti, Luca M. Gambardella, Jürgen Schmidhuber "Mitosis Detection in Breast Cancer Histology Images with Deep Neural Network" MICCAI 2013: Medical Image Computing and Computer-Assisted Intervention – MICCAI 2013 pp 411-418
16. Shadi Albarqouni, Christoph Baur, Felix Achilles, Vasileios Belagiannis, Stefanie Demirci, Nassir Navab "Aggnet: Deep learning from crowds for mitosis detection in breast cancer histology images" IEEE Transactions on Medical Imaging ,vol 5, 1313-1321, 2016
17. Yao Xue, Nilanjan Ray "Cell Detection in Microscopy Images with Deep Convolutional Neural Network and Compressed Sensing" Computer Vision and Pattern Recognition, in CVPR, 2017
18. Uwe Schmidt, Martin Weigert, Coleman Broaddus, Gene Myers "Cell Detection with Star-convex Polygons" in MICCAI, 2018
19. Wahlby C, Lindblad J, Vondrus M, Bengtsson E, Bjorkesten L. "Algorithms for cytoplasm segmentation of fluorescence labelled cells." Anal Cell Pathol: J Eur Soc Anal Cell Pathol. 2002;24(2):101–11.
20. Wang M, Zhou X, Li F, Huckins J, King RW, Wong STC. "Novel cell segmentation and online SVM for cell cycle phase identification in automated microscopy." Bioinformatics. 2008;24(1):94–101.
21. Sharif JM, Miswan MF, Ngadi MA, Salam MSH, Jamil MMbA. "Red blood cell segmentation using masking and watershed algorithm: A preliminary study." In: 2012 International Conference on Biomedical Engineering (ICoBE); 2012. p. 258–62.
22. Nath SK, Palaniappan K, Bunyak F. "Cell segmentation using coupled level sets and graph-vertex coloring." In: International Conference on Medical Image Computing and Computer-Assisted Intervention; 2006. p. 101–8.
23. Dzyubachyk O, Niessen W, Meijering E. "Advanced level-set based multiple-cell segmentation and tracking in time-lapse fluorescence microscopy images." In: 2008 5th IEEE International Symposium on Biomedical Imaging: From Nano to Macro; 2008. p. 185–8.
24. Dorini LB, Minetto R, Leite NJ. "White blood cell segmentation using morphological operators and scale-space analysis." In: XX Brazilian Symposium on Computer Graphics and Image Processing (SIBGRAPI 2007); 2007. p. 294–304.
25. Wang X, He W, Metaxas D, Mathew R, White E. "Cell segmentation and tracking using texture-adaptive shakes." In: 2007 4th IEEE International Symposium on Biomedical Imaging: From Nano to Macro; 2007. p. 101–4.
26. Van Valen DA, Kudo T, Lane KM, Macklin DN, Quach NT, DeFelice MM, Maayan I, Tanouchi Y, Ashley EA, Covert MW. "Deep learning automates the quantitative analysis of individual cells in live-cell imaging experiments." PLoS Comput Biol. 2016; 12(11): 1005177–124.
27. Kraus OZ, Grys BT, Ba J, Chong Y, Frey BJ, Boone C, Andrews BJ. "Automated analysis of high-content microscopy data with deep learning. " Mol Syst Biol. 2017;13(4):924.
28. Ronneberger, O., Fischer, P., Brox, T. "U-net: Convolutional networks for biomedical image segmentation." In: MICCAI (2015)
29. Jean-Baptiste Lugagne, Haonan Lin, Mary J. Dunlop "DeLTA: Automated cell segmentation, tracking, and lineage reconstruction using deep learning" PLoS Comput Biol. 2020 Apr; 16(4): 1007673.